



Thresholding Techniques for Image Denoising and Their Comparison by Different Wavelets

**Malati Mazumder^{1*}, Md. Shahadat Hossain², Md. Asaduzzaman³
and Md. Rafiqul Islam²**

¹*Department of Applied Mathematics, Gono Bishwabidyalay, Dhaka-1344, Bangladesh.*

²*Mathematics Discipline, Science, Engineering and Technology School, Khulna University,
Khulna-9208, Bangladesh.*

³*Department of Computer Science and Engineering, North Western University, Khulna, Bangladesh.*

Authors' contributions

This work was carried out in collaboration between all authors. Author MM designed the study, captured the images required for the study, performed the statistical analysis and wrote the protocol. Author MSH wrote the first draft of the manuscript, decorated it, managed the analyses of the study, managed the literature searches and modified the bibliographic arrangements. Author MA contributed in decorating the references along with some logical assistances. Author MRI provided proper logistic supports. All authors read and approved the final manuscript.

Article Information

DOI: 10.9734/CJAST/2018/42217

Editor(s):

(1) Samir Kumar Bandyopadhyay, Professor, Department of Computer Science and Engineering, University of Calcutta, India.

Reviewers:

(1) Anonymous, Siddaganga Institute of Technology, India.

(2) Zlatin Zlatev, Trakia University, Bulgaria.

Complete Peer review History: <http://www.sciencedomain.org/review-history/25985>

Original Research Article

Received 19th May 2018
Accepted 7th August 2018
Published 24th August 2018

ABSTRACT

Though the digital images are considered as the medium of transmitting visual information and crucial technique of modern communication, the obtained images sometimes may be corrupted by unexpected noise. However, these noisy images require further processing, which involves the manipulation of the image data to produce a visually high-quality image. In this paper, several thresholding techniques, namely SureShrink, VisuShrink and BayeShrink have been presented and the suitable one is determined. In addition, various noise models, for instance, Gaussian noise, salt and pepper noise and speckle noise, along with additive and multiplicative types have been utilized. The selection of the denoising algorithm being application dependent, it is crucial to have proper knowledge regarding the noise in each image for the purpose of selecting the appropriate algorithm. Typically, the wavelet-based approach finds applications in denoising images corrupted with Gaussian noise. Here the mean square error of the images has been determined as a quantitative measure.

*Corresponding author: E-mail: malati051205@yahoo.com;

Keywords: Image denoising; DWT; SureShrink; VisuShrink; BayesShrink; Thresholding.

1. INTRODUCTION

Discussing the image analysis is related to representing a signal which was, at first, introduced by Joseph Fourier [1]. Following him, another prominent mathematician Alfred Haar [2], in 1909, developed the theory of wavelet in his PhD thesis. Besides, Edwards [3] described DWT. In addition, Paul Levy, 1930s found the scale-varying Haar basis function superior to Fourier basis functions. The concept of wavelets in its present theoretical form was, at first, proposed by Jean Morlet and Alex Grossman (continuous wavelet transform, 1982).

Furthermore, the methods of wavelet analysis have been developed mainly by Meyer [4], whereas, Mallat [5] developed a multiresolution analysis using wavelets. Afterwards, Daubechies [6,7] used the theory of multiresolution wavelet analysis to construct her own family of wavelets. Her set of wavelet orthonormal basis functions has become the cornerstone of wavelet applications today. With her work, the theoretical treatment of wavelet analysis is as much as covered.

Wavelet is, now, being implemented as an indispensable tool for a numerous purpose, namely data analysis, image processing, signal processing [8,9,10] including compression and denoising, where, for example, discretely sampled time-series data might need to be analysed [11]. Typically, there exists noise in the signal during its preservation, which is likely to be erased with the help of wavelet denoising, regardless of its frequency content [12]. Wavelet thresholding, first proposed by Donoho [13], is a procedure for estimating signal that boosts the signal denoising using wavelet transform. It alleviates the insignificant noises, turning out it to be simple and effective, and relays significantly on the choice of the thresholding parameter along with the threshold determines [14]. Winkler [15], in 1995, introduced Monte Carlo methods to analyse the image, where Diego Maldonado (2009) for denoising.

Diversified research works have been conducted throughout the world, for instance, Xiao and Zhang [16], in 2011, explored the properties of several representative thresholding techniques, such as VisuShrink, SureShrink, BayesShrink and Feature Adaptive Wavelet Shrinkage [17]. In addition, the optimal threshold can be estimated from the image statistics for getting better

performance of denoising in terms of clarity or quality of the images. Besides, Saurabh [18] illustrated image denoising from the sonar image by using VishuShrink, BayesShrink and NeighShrink experimentally and compared the result in terms of various image quality parameters (PSNR, MSE, SSIM and Entropy). On top of that, Gauhathakurta [19] used wavelet time to determine the best one for image denoising, where MSE and PSNR have been measured as a quantitative performance tool. Nigam [20] studied four different thresholding techniques (Visual Shrink, Normal or Bayesian Shrink, Neighbour Shrink and Modified Neighbour Shrink) in order to denoise image in the wavelet domain [21]. Visual and Normal Shrink is independent of window size, whereas the other two shrinks are not. The use of available biorthogonal wavelets in image denoising is typically less common because of their poor performance. To eradicate this impediment, Pragada [22] presented a method to design an image-matched biorthogonal wavelet bases and report on their potential for denoising.

Taking everything into consideration a technique is proposed in this paper, which is likely to eliminate the complexities of denoise image successfully compared to the existing techniques.

2. SUMMARY OF METHODS FOR DENOISING IMAGE ANALYSIS

There are numerous procedures for restoring an image from noisy distortions [12]. The denoising methods tend to be problem specific, for instance, a technique to denoise satellite images may not be perfect for denoising medical images. A high-quality image is used for the purpose of quantifying the performance of diversified denoising algorithms, and at the same time, the noise adds to it [12]. Consequently, an input is provided to the denoising algorithm, which produces an image approximately the same as an original high-quality image. Afterwards, MSE, as well as the visual interpretation, are computed for comparing the performance of each algorithm.

It requires to be well-known to the characteristics of the degrading system along with the noises, at first, for a successful image denoising method [12]. The "Linear operation" as shown in the following Fig. 1, the image $s(x,y)$ is blurred by a

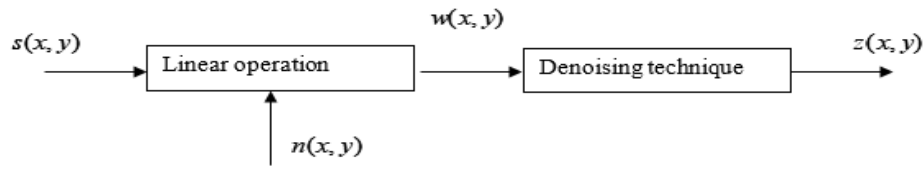


Fig. 1. Denoising concept [12]

linear operation and noise $n(x, y)$ is added to form the degraded/corrupted image $w(x, y)$, which is then convolved with the restoration procedure $g(x, y)$ to produce the restored image $z(x, y)$ [12].

A threshold is a fixed value such that all the coefficients that are larger than this value are kept and ones smaller than it is zero out. So, by thresholding wavelet coefficients, are simply removing coefficients smaller than the threshold by setting them equal to zero. There are many schemes of thresholding. In this report, we will be discussing such schemes, namely soft thresholding, hard thresholding, VisuShrink, SureShrink, and BayesShrink thresholding.

3. DIFFERENT KINDS OF NOISE (GAUSSIAN NOISE)

Gaussian noise is evenly distributed over the signal, where each pixel in the noisy image is constructed using the sum of the true pixel value and a random Gaussian distributed noise value [12]. Typically, Gaussian distribution has a bell-shaped probability distribution function [12] given by,

$$F(g) = \frac{1}{\sqrt{2\pi\sigma^2}} e^{-\frac{(g-m)^2}{2\sigma^2}}$$

Where, g , m and σ are represented as, respectively, grey level, the mean of the function and standard deviation of the noise. The graphical representation of the Gaussian distribution is shown in Fig. 2.

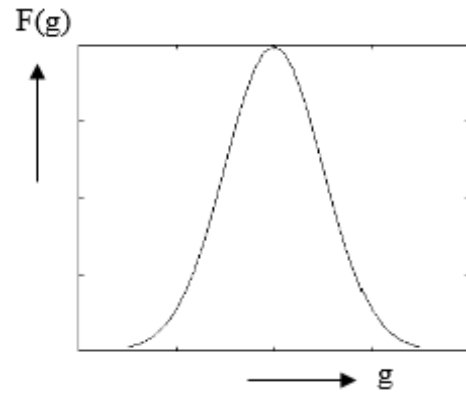


Fig. 2. Gaussian distribution [12]

On an image, Gaussian noise (with variance 0.05) looks as shown in Image.

3.1 Salt and Pepper Noise

Salt and pepper noise, also referred to as intensity spikes, is generally considered an impulse type of noise, which is caused by errors in data transmission [12]. It has only two possible values, namely a and b , where the probabilities are individually less than 0.1. The corrupted pixels are alternately set to the minimum or maximum value, which gives an image a “salt and pepper” like appearance. For an 8-bit image, the typical value of pepper noise is 0 and for salt noise 255. From various studies, it has been explored that maximum noises are generally caused by malfunctioning of pixel elements in the camera sensors, faulty memory locations, or timing errors in the digitization process.



Fig. 3. Original and Gaussian noise image with mean=0 and variance=0.05

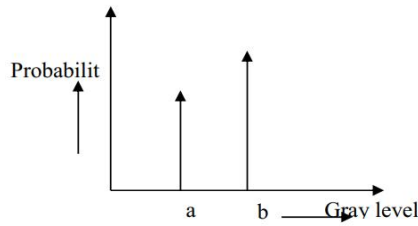


Fig. 4. Salt and Pepper noise [12]

The probability density function for this type of noise is shown in Figure. Salt and pepper noise with a variance of 0.05 is shown in Image.

3.2 Speckle Noise

The source of speckle noise [23], which is multiplicative, and occurs, in maximum coherent

imaging systems, namely laser, acoustics and SAR (Synthetic Aperture Radar) imagery, is attributed to random interference between the coherent returns [24]. And the most interesting point should be mentioned is that Speckle noise is basically defiled, in accordance with a gamma distribution, as follows

$$F(g) = \frac{g^{\alpha-1}}{(\alpha-1)!a^\alpha} e^{-\frac{g}{a}}, \text{ where variance is } a^2\alpha \text{ and } g \text{ is the grey level.}$$

The gamma distribution is given below in Fig. 6.

On an image, speckle noise (with variance 0.05) looks as shown in Image.



Fig. 5. Salt and pepper noise with variance 0.05

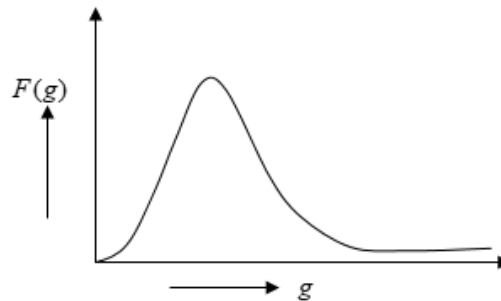


Fig. 6. Gamma distribution



Fig. 7. Speckle noise with variance 0.05

4. VARIOUS TYPES OF IMAGE SHRINKING

4.1 VisuShrink

VisuShrink, introduced by Donoho [13], follows the hard thresholding rule, which is, in addition, referred to as a universal threshold and is defined as

$$t = \sigma\sqrt{2\log n} \quad (1)$$

Where σ^2 and n represent respectively the noise variance existing in the signal and signal size (number of samples) [25]. An estimate of the noise level σ depending on the median absolute deviation [26] given by

$$\hat{\sigma} = \frac{\text{midian}\left(\left\{g_{j-1,k} : k = 0,1,\dots,2^{j-1} - 1\right\}\right)}{0.6745} \quad (2)$$

Where $g_{j-1,k}$ corresponds to the detail coefficients in the wavelet transform [25].

VisuShrink, instead of minimizing the MSE, can be used as a thresholding technique that shows near optimal minimax error properties and provides with high probability that the estimates are as smooth as the true underlying functions [25]. Typically, VisuShrink removes too many coefficients. So, it is known as overly smoothed yield recovered image. Another drawback is the speckle noise, which can't be effortlessly erased, and only additive noise can be dealt with [25]. VisuShrink follows the global thresholding scheme, where a single value of the threshold is globally applied to all the wavelet coefficients.

4.2 SureShrink

The SureShrink, a combined form of universal threshold and SURE (Stein's Unbiased Risk Estimator) threshold, was firstly introduced by Donoho and Johnstone [27]. This method specifies a threshold value t_j for each resolution level j in the WT, which is referred to as level dependent thresholding [28]. The principal aim of SureShrink is to minimize the MSE and is defined as

$$\text{MSE} = \frac{1}{n^2} \sum_{x,y=1}^n [z(x,y) - s(x,y)]^2 \quad (3)$$

where $z(x,y)$ represents the signal estimate, while $s(x,y)$ denotes the original signal without noise and n is considered as the signal size. SureShrink suppresses noise by thresholding the empirical wavelet coefficients. The SureShrink threshold t^* is defined as $t^* = \min(t, \sigma\sqrt{2\log n})$

where, t denotes the value that minimises SURE, σ represents the noise variance computed from Equation (2), and n is the image size. SureShrink, soft thresholding employed here, is adaptive in the sense that a threshold level is assigned to each dyadic resolution level by the principle of minimising the SURE for threshold estimates [28]. Furthermore, it is smoothness adaptive, which means that if the unknown function contains abrupt changes or boundaries in the image, the reconstructed image also does.

4.3 BayesShrink

BayesShrink was proposed by Chang *et al.* [29] for minimizing the Bayesian risk. The BayesShrink basically uses the soft thresholding, relies on subband, which means that thresholding is accomplished at each band of resolution in the wavelet decomposition [25]. Like the SureShrink, it is smoothness adaptive, which is defined as

$$t_B = \sigma^2 / \sigma_s \quad (4)$$

where σ^2 and σ_s^2 are respectively the noise variance and signal variance without noise. The value of the noise variance σ^2 is determined from the subband HH1 by the median estimator [25] as shown in the Equation (4). In this task, the adaptive noise is defined as $w(x,y) = s(x,y) + n(x,y)$

In general, the noise and the signal are independent of each other [25], it can be stated that

$$\sigma_w^2 = \sigma_s^2 + \sigma^2$$

$$\sigma_w^2 \text{ can be computed as } \sigma_w^2 = \frac{1}{n^2} \sum_{x,y=1}^n w^2(x,y)$$

The variance of the signal is computed as

$$\sigma_s = \sqrt{\max(\sigma_w^2 - \sigma^2, 0)} \quad (5)$$

with σ^2 and σ_s^2 the Bayes threshold is determined from Equation (3).

BayesShrink has been experimented to remove Gaussian noise (mean=0, variance = 0.05) and speckle noise (variance = 0.05). The input and output images after applying BayesShrink can be seen in the Figs. 12 to 15.



Fig. 8. Image corrupted with Image Gaussian Noise, Variance 0.005



Fig. 9. Image after applying VisuShrink



Fig. 10. Input corrupted with Image Gaussian Noise



Fig. 11. Image after SureShrink Thresholding



Fig. 12. Image corrupted with Image Gaussian Noise

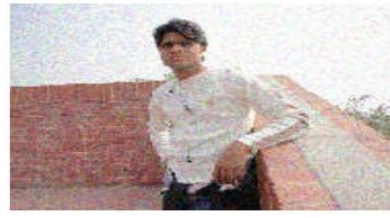


Fig. 13. Image subjected to BayesShrink



Fig. 14. Image corrupted with Image speckle noise



Fig. 15. Image subjected to BayesShrink

5. RESULTS AND DISCUSSION

In statistics, the MSE of an estimator is a way to quantify the difference between values implied by a kernel density estimator and the true values of the quantity being estimated. MSE is a risk function, corresponding to the expected value of the squared error loss or quadratic loss. The error is the amount by which the value implied by the estimator differs from the quantity to be estimated.

The MSE is the second moment of the error, and in this way, it incorporates both the variance of the estimator and its bias, whereas, for an unbiased estimator, the MSE is considered as the variance. Because MSE, just like the variance, is measured with the same units as the square of the quantity being estimated.

In statistical modelling, the MSE, which sometimes indicate minimal variance, is used to determine to what extent the model does not fit the data, or whether removing certain terms could simplify the model in beneficial ways. Taking the square root of MSE yields the Root Mean Square Deviation, which is a good measure of precision, and is also known as the Quadratic Mean. Having an MSE of zero (0) is ideal, but in most situations never possible. An MSE of 0 means the estimator predicts observations with perfect precision. The measure of this error outlined in this paper is the square Euclidean norm

$$\|F - \tilde{F}\|^2 = \sum_{n_1=1}^M \sum_{n_2=1}^N [F(n_1, n_2) - \tilde{F}(n_1, n_2)]^2 ,$$

which is fairly simple and accurate in most cases.

Mean square error (MSE) also gives a measure of this error which is defined as

$$MSE = \frac{1}{MN} \|F - \tilde{F}\|^2 = \frac{1}{MN} \sum_{n_1=1}^M \sum_{n_2=1}^N [F(n_1, n_2) - \tilde{F}(n_1, n_2)]^2$$

The denoising process of the image was observed using a number of different wavelets, namely, Daubechies 4, Haar, available in MATLAB. It is quite evident from the summary that the tables they are almost the same for these different wavelets. Since these wavelets have different shapes and sizes, they will capture the different local features of the image. Since these subtle local features vary from image to image, the superiority of wavelet over another cannot be concluded, which is so much convenient beyond the comparison purposes. From the summary tables, it can be compared the denoising image for different thresholding techniques of different wavelets and calculate the MSE.

5.1 A Thresholding Scheme with Gaussian Noise

Visu Shrink



Fig. 16. The original image, a noisy image with Gaussian noise (0.05), denoising image (VisuShrink) with Daubechies 4



Fig. 17. The original image, a noisy image with Gaussian noise (0.05), denoising image (VisuShrink) with Haar

Table 1. Summary of denoising result for an image of Man with Daubechies 4 and Haar

Method	MSE of the output image	Noise type and variance, σ
VisuShrink with Daubesies 4	8.1719e+007	Gaussian, 0.05
	8.3084e+007	
	8.3142e+007	
VisuShrink with Haar	8.2546e+007	
	8.3948e+007	
	8.4693e+007	

SureShrink



Fig. 18. The original image, a noisy image with Gaussian noise (0.05), denoising image (SureShrink) with Daubechies 4



Fig. 19. The original image, a Noisy image with Gaussian noise (0.05), Denoising image (SureShrink) with Haar

Table 2. Summary of denoising result for an image of Man with Daubechies 4 and Haar

Method	MSE of the output image	Noise type and variance, σ
SureShrink with Daubesies 4	1.1793e+007	Gaussian, 0.05
	2.2922e+007	
	2.2828e+007	
SureShrink with Haar	1.2726e+007	
	2.5013e+007	
	2.4539e+007	

BayesShrink thresholding scheme



Fig. 20. The original image, a Noisy image with Gaussian noise (0.05), Denoising image (BayesShrink) with Daubechies 4



Fig. 21. The original image, a Noisy image with Gaussian noise (0.05), Denoising image (BayesShrink) with Haar

Table 3. Summary of denoising result for an image of Man with Daubechies 4 and Haar

Method	MSE of the Output image	Noise type and variance, σ
BayesShrink with Daubesies 4	1.0144e-016	Gaussian, 0.05
	1.1045e-016	
	1.1325e-016	
BayesShrink with Haar	1.6922e-022	
	1.5122e-022	
	1.4750e-022	

5.2 Denoising with Gaussian Noise, and Salt and Pepper Noise

VisuShrink



Fig. 22. The original image, a Noisy image with Gaussian noise (0.05), De noising image (VisuShrink) with Haar

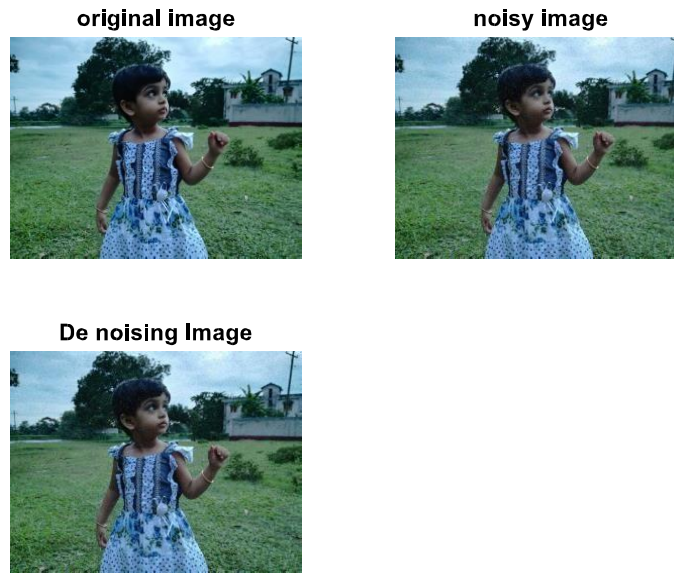


Fig. 23. The original image, a noisy image with salt & pepper noise (0.05), denoising image (VisuShrink) with Haar

Table 4. Summary of denoising result for Image with Haar

Method	MSE of Output image	Noise type and variance, σ
VisuShrink	9.7016e+10 1.0278e+11 9.3558e+10	Gaussian, 0.05
VisuShrink	458091552 5.0843e+08 5.3128e+08	Salt & Pepper, 0.05

SureShrink



Fig. 24. The original image, noisy image with Gaussian noise (0.05), denoising image (SureShrink) with Haar



Fig. 25. The original image, a noisy image with salt & pepper noise (0.05), denoising image (SureShrink) with Haar

Table 5. Summary of denoising result for Image with Haar

Method	MSE of output image	Noise type and variance, σ
SureShrink	1.5886e+10	Gaussian, 0.05
	2.8635e+10	
	2.7645e+10	
SureShrink	1.1254e+08	Salt & Pepper, 0.05
	202482896	
	202318048	

BayesShrink



Fig. 26. The original image, a noisy image with Gaussian noise (0.05), denoising image (BayesShrink) with Haar

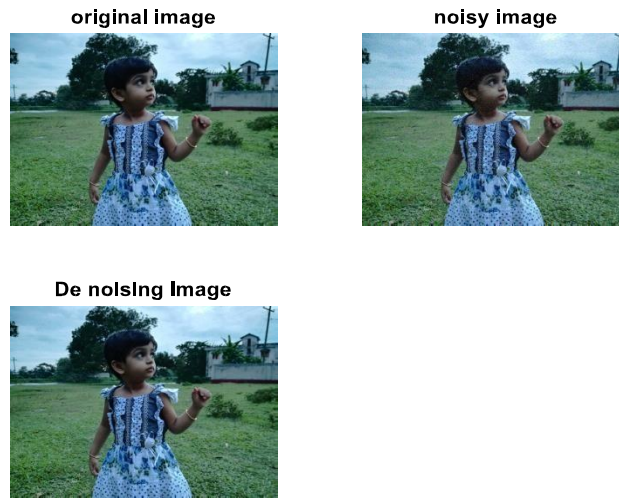


Fig. 27. The original image, a noisy image with salt & pepper noise (0.05), denoising image (BayesShrink) with Haar

Table 6. Summary of denoising result for Image with Haar

Method	MSE of output image	Noise type and variance, σ
BayesShrink	3.8853e-28	Gaussian, 0.05
	6.0722e-28	
	5.8397e-28	
BayesShrink	3.1255e-28	Salt & Pepper, 0.05
	5.5843e-28	
	5.2411e-28	

6. CONCLUSIONS

6.1 Summary of Achievements

Image processing technique that has been studied, is image denoising via thresholding on the basis of the various wavelet, namely Daubechies 4 and Harr wavelet MATLAB. The original images of different persons, corrupted with some randomly generated Gaussian noise or Salt and Pepper noise, have been used in this paper. Three different thresholding schemes, namely, VisuShrink, SureShrink, BayesShrink thresholding has been selected to detect local features for comparison. However, the denoising results can be easily compared with Daubechies 4 and Haar wavelets for different thresholding techniques. The result shows that BayesShrink thresholding, which is more sophisticated compared to others performs consistently the best as it has the lowest MSE value.

6.2 Future Works

The selection of the congenial denoising technique plays the crucial role, and this is because it is significant to explore and

accomplish a comparison among the methods. It is expected that various denoising techniques would likely to implement in neural network and pattern recognition through feeding the denoised signal, which is anticipated to determine the rate of successful classification. On top of that, impediments can be to the time flops of the CPU computing, which may generate a barrier of time complexity standard for each algorithm. The aforementioned two points would be taken into consideration for an extension of the present work done.

DISCLAIMER

The images used in this research work were captured using a manually operated camera, and no editing task was accomplished. Besides, all the images were taken completely in the natural environment, instead of any artificial mode to intensify the resolution/quality of the images.

ACKNOWLEDGEMENTS

Special credit goes to Professor Dr. Md Rafiqul Islam, a mentor while accomplishing this

research work, who provided logistic supports and special suggestions from the beginning to the culmination.

COMPETING INTERESTS

Authors have declared that no competing interests exist.

REFERENCES

1. The Fourier Transform. Available:<http://thefouriertransform.com/>
2. The Wavelet Transform. Available:<http://gwyddion.net/documentation/user-guide-en/wavelet-transform.html>
3. Edwards T. Discrete wavelet transforms: Theory and implementation. Discrete Wavelet Transforms, Stanford University, Draft #2; 1992.
4. Meyer Y. Wavelets, Algorithms and Applications, Edited by Ryan), Robert D. SIAM Publications; 1993.
5. Mallat S. Multiresolution representation and wavelets, University of Pennsylvania. PhD Thesis; 1988.
6. Daubechies I. Ten lectures on wavelets, SIAM, Philadelphia; 1992.
7. Daubechies I. Recent results in wavelet applications. Journal of Electronic Imaging. 1998;7(4):1.
8. Castleman KR. Digital image processing, Prentice Hall, New Jersey; 1996.
9. Niblack W. An introduction to digital image processing, Prentice Hall, New Jersey; 1986.
10. Image processing fundamentals-statistics. Signal to Noise Ratio; 2001.
11. Graps A. An introduction to wavelets. IEEE Computational Science and Engineering, Summer. 1995;2(2).
12. Avni K. Enhanced images using noise removal with image restoration. IJSRD - International Journal for Scientific Research & Development. 2015;3(3):2244-2249.
13. Donoho DL. De-noising by soft-thresholding, in IEEE Transactions on Information Theory. 1995;41(3):613-627.
14. Sudharani B. A better thresholding technique for image denoising based on wavelet transform. International Journal of Innovative Research in Computer and Communication Engineering. 2015;3(5): 4608-4615.
15. Winkler G. Image analysis, random fields and dynamic Monte Carlo methods: A mathematical introduction, Springer-Verlag Berlin Heidelberg. 1995;324.
16. Xiao F, Zhang Y. A comparative study on thresholding methods in wavelet-based image denoising. Procedia Engineering. 2011;15:3998-4003.
17. Taswell C. The what, how, and why of wavelet Shrinkage denoising. Technical Report, Stanford, CA; 1999.
18. Saurabh A, Kumar A, Anitha U. Performance analysis of various wavelet thresholding techniques for despeckling of sonar images. 2015 3rd International Conference on Signal Processing, Communication and Networking (ICSCN), Chennai. 2015;1-7.
19. Guhathakurta R. Denoising of image: A wavelet-based approach, 2017 8th Annual Industrial Automation and Electromechanical Engineering Conference (IEMECON), Bangkok, 2017; 194-197.
20. Nigam V, Luthra S, Bhatnagar S. A comparative study of thresholding techniques for image denoising, 2010 International Conference on Computer and Communication Technology (ICCT), Allahabad, Uttar Pradesh. 2010;173-176.
21. Shrivastava S, Dubey R, Kerhalker SG, Image Denoising using Multilevel Filtering Approach. IOSR Journal of Electrical and Electronics Engineering (IOSR-JEEE). 2014;9(4):22-27.
22. Pragada S, Sivaswamy J, Image denoising using matched biorthogonal wavelets. 2008 Sixth Indian Conference on Computer Vision, Graphics & Image Processing, Bhubaneswar. 2008;25-32.
23. Gagnon L. Wavelet filtering of speckle noise-some numerical results, Proceedings of the Conference Vision Interface; 1999, Trois-Riveres.
24. Gupta MB, Negi MSS. Image denoising with linear and non-linear filters: A Review. IJCSI International Journal of Computer Science Issues. 2013;10(6):149-154.
25. Uppal KK, Kumar A. Denoising of image and its performance evaluation. IOSR Journal of Electrical and Electronics Engineering (IOSR-JEEE). 2014;9(2):80-82.
26. Donoho DL. Statistical estimation and optimal recovery. The Annals of Statistics. 1994;22(1):238-270.

27. Donoho DL, Johnstone IM. Adapting to unknown smoothness via wavelet shrinkage. *Journal of American Statistical Association*. 1995;90(432):1200-1224.
28. Vohra R, Tayal A. Image restoration using thresholding techniques on wavelet coefficients. *IJCSI International Journal of Computer Science Issues*. 2011;8(5):400-4404.
29. Chang SG, Yu B, Vetterli M. Adaptive wavelet thresholding for image denoising and compression, *IEEE Transaction on Image Processing*. 2000;9(9):1532-1546.

© 2018 Mazumder et al.; This is an Open Access article distributed under the terms of the Creative Commons Attribution License (<http://creativecommons.org/licenses/by/4.0>), which permits unrestricted use, distribution, and reproduction in any medium, provided the original work is properly cited.

Peer-review history:
The peer review history for this paper can be accessed here:
<http://www.sciencedomain.org/review-history/25985>